This article has been accepted for publication in a future issue of this journal, but has not been fully edited. Content may change prior to final publication. Citation information: DOI 10.1109/TTE.2021.3052106, IEEE Transactions on Transportation Electrification

Future of Electrical Aircraft Energy Power Systems: An architecture review.

Tania C. Cano[1], *Student member, IEEE*, Alberto Rodríguez[1], *Member, IEEE,* Diego G. Lamar[1], *Senior Member, IEEE,* Ignacio Castro[2], *Member, IEEE,* Laura Albiol-Tendillo[2], *Member, IEEE,* Yehia F. Khalil[3] and Parag Kshirsagar[4], *Senior Member, IEEE*.

***Abstract*— This paper presents and in-depth analysis of All-Electric-Aircraft (AEA) architectures. The aim of this work is to provide a global vision of the current AEA state of art, to estimate main technological gaps and drivers and to identify the most promising architecture configuration for future electrical aircraft in the context of a twin propeller 20 MW aircraft. The comparison between architectures is done based on three different figures of merit: reliability, efficiency and specific power density. The methodology presented and the trade studies are applied to a narrowbody aircraft of 20 MW, equivalent to an Airbus A320, and following current efforts of government agencies to achieve cleaner air mobility within the next two decades.**

***Index Terms*— Aerospace electronics, Aircraft propulsion, Air transportation, Turbogenerators, Hybrid power systems, Power system planning, Fault tolerance, Redundancy.**

I. Introduction

THE contribution of the aerospace sector to CO_2 global emissions amounts to 2.4% and it is expected to continue increasing due to the constant growth of the sector, where passenger operation aviation is the main source of CO_2 emissions. In 2018, the International Air Transport Association (IATA) forecasted that the civil aviation industry will grow at a 3.5% rate for the next two decades [1] The impact of COVID-19 on aerospace industry may reduce this prospect momentarily but efficient and greener solutions are of utter importance for the sector.

Fig. 1 shows a classification of commercial aircraft CO_2 emissions by operation and subdivided in aircraft classes [2]. Passenger operation is responsible for the majority of CO_2 emissions (81%) and it is divided into three aircraft classes: narrowbody or single-aisle aircraft refers to aircrafts up to 295 passengers, widebody or two-aisle aircraft refers to aircraft between 250 and 600 passengers, and regional aircraft refers to short-haul flights up to 100 passengers. Freight operation includes two aircraft classes. Dedicated freight or cargo aircraft (i.e., designed for the carriage of cargo), and belly freight, that refers to the use of passenger aircraft deck for air cargo. As can be seen, narrowbody passenger aircraft class and widebody amount to 76% of the total CO_2 emissions generated by commercial aircraft. Thus, emission reduction strategies focus their effort on studying those classes. The present work is focused on commercial narrowbody passenger aircraft class but it could be extended to the widebody passenger class. Military aviation has not been included in the presented classification. A study estimates military jet fuel amounts to 6.7% of commercial aviation emissions in 2018 [2]. Additionally, Boston University has recently published a study about the Pentagon fuel used where the impact of the US department of defense (DOD) in global CO_2 emissions is reported. It is estimated that the 71% of the DOD energy used correspond to air domain [3].

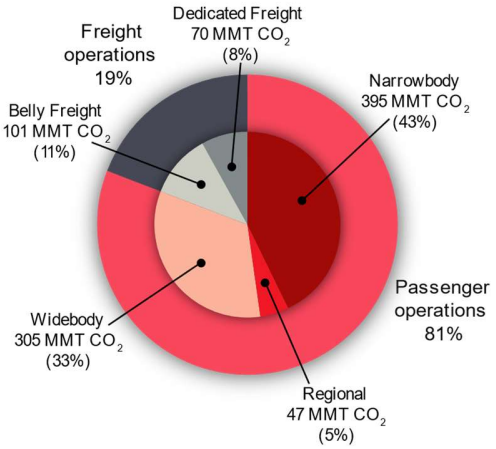

Fig. 1. CO_2 emissions generation by the aerospace sector and classified by operations and aircraft classes (2018 data). CO_2 is expressed in Million Metric Tonnes (MMT) [2]

Long-term roadmaps such as Advisory Council for Aeronautics Research in Europe (ACARE) Flightpath 2050 [4], aim to reduce CO_2 emission per passenger kilometer by 75% and 90% reduction of NO_x. Worldwide research programs, such as Clean Sky [5], encourage the development of innovative aircraft technologies [6]. Achieving these strategic goals

* This work was supported by the European Union's Horizon 2020 research and innovation program under grant agreement No 875504 and the spanish government (CIU-19-RTI2018-099682-A-I00).

[1] T.C.Cano, A.Rodriguez, D.G.Lamar are with the Power Supply Group, University of Oviedo (e-mail: cuestacanotania.fuo@uniovi.es).

[2] Ignacio Castro, L. Albiol-Tendillo are with Raytheon Technologies Research Center, Cork (e-mail:ignacio.castro@rtx.com, laura.albiol-tendillo@rtx.com).

[3] Yehia F. Khalil is with Connecticut Academy of Science & Engineering (CASE). (e-mail: ykhalil@alumni.stanford.edu).

[4] Parag Kshirsagar is with Raytheon Technologies Research Center, E. Hartford (e-mail: parag.kshirsagar@rtx.com)

This article has been accepted for publication in a future issue of this journal, but has not been fully edited. Content may change prior to final publication. Citation information: DOI 10.1109/TTE.2021.3052106, IEEE Transactions on Transportation Electrification

requires reconsideration of the underlying concepts of traditional aircrafts, which have not changed since the 1950s. However, the required changes are not limited to the architecture, the building blocks for electrical/hybrid propulsion need to be explored, as major technology breakthroughs are required to achieve the expected benefits of electrical aviation.

The electrical distribution system of previous generation commercial aircraft supplies avionics and secondary loads, see Fig. 2 .a. These loads comprise hotel and galley loads, cabin lights, etc. and typically amount to a few kWs. In the last years, there has been an increase in the effort of electrification of pneumatic and hydraulics systems for improving aircraft system efficiency, although the idea is not such new [7], see Fig. 2 .b. These extra electric loads have increased the power consumption to hundreds of kWs dividing the aircraft in several power sections and have given rise to the More-Electric-Aircraft (MEA) concept. Airbus A380 and Boeing 787 are some examples of MEA. The MEA Energy Power System (EPS) must manage higher power demand keeping low weight, high efficiency, and high reliability characteristics. Most promising MEA EPS architectures are analyzed and compared in [8].

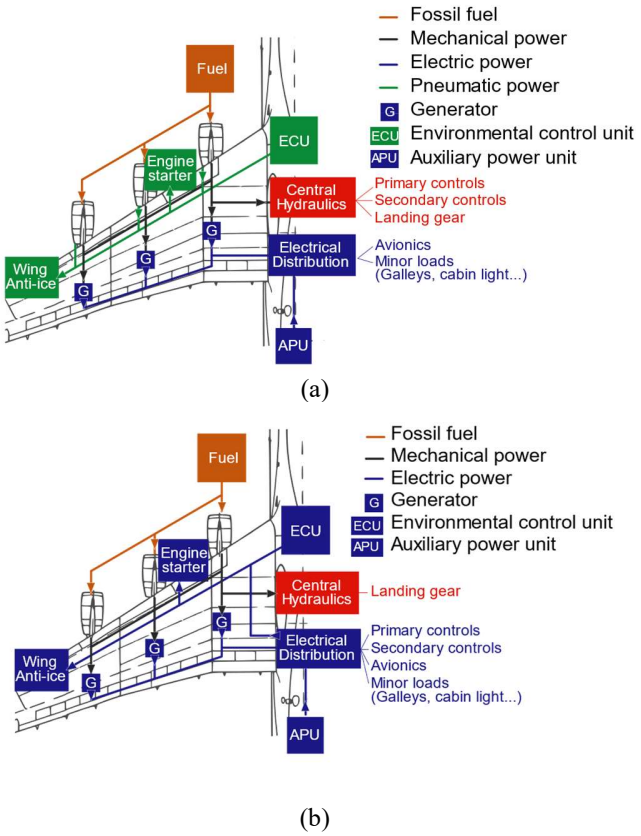

Fig. 2. On board power systems in current commercial Aircraft (a) and in a MEA (b).

Efforts on MEA have enhanced efficiency, reduced weight, improved comfortability of passengers and set a new paradigm in aviation systems. However, they are not enough to achieve the required emission reduction for future decades [4].

Therefore, the next steps are aimed at greener aircraft able to provide the same operation with reduced emission [9]. This can be achieved by increasing the electrification efforts and aiming at full or hybrid electric aircrafts, or by achieving operation with more sustainable fuels, such as, hydrogen or bio-fuels [11]–[14]. This paper will focus on replacing conventional fuel-based propulsion systems by electric alternatives and comparing their effectiveness. The utilization of full and hybrid electric propulsion for aircraft has been referred in recent years as All-Electric-Aircraft (AEA) [14]. Fig. 3 represents different high level schematics of AEA based on [16]– [18] and which can be categorized as follow:

a) Parallel hybrid: the electric motor is connected to the low-pressure spool of the turbine. Either or both gas turbine and motor driven fan can provide propulsive thrust independently [18], [19].
b) Series hybrid: the turboshaft drives an electric generator; this electric power is used to either drive the propulsion engines or charge an energy storage system (ESS). ESS also support power demand when required [20].
c) Series/Parallel hybrid: it combines mechanically driven and electrically driven fans. The latter ones can be powered by the turboshaft generator or ESS.
d) All turboelectric: the turboshaft power is used to drive an electric generator. This electric power is used to drive motor driven fans.[21].
e) Partial turboelectric: the turbofan provides both thrust and electric generator driven roles. The rest of the thrust is produced by motor driven fans.[23].
f) All electric: the ESS drives electrically the propulsion engines. ESS can be charged or replace when aircraft is on the ground [23], [24].

Increasing electrical power consumption from a hundred of kWs in MEA toward MW level AEA EPS design is not trivial and several figures of merit (FoM) need to be defined to correctly quantify which are the requirements for both the system and the building blocks, such as efficiency, specific power (kW/kg) or reliability (Failures in Time, FITs).The design of MW AEA EPS involves solving several challenges related to the volume of power required for these aircrafts, which be summarized by, how do we make the EPS lossless, compact and weightless to achieve zero fuel dependency or significant fuel savings. This comment translates into tackling several technological challenges: high voltage distribution, superconductivity, thermal management and power generation [25].

High voltage, at kV level, is required for MW applications to reduce otherwise extremely high current levels. The introduction of HV MW AEA EPS distribution systems brings new concerns related to HV challenges, such as, partial discharge, serial arc and space charge. Although, these phenomena have been solved in ground applications, for aviation due to the weight and volume restrictions and air density conditions due to high altitude, are yet to be solved. For MEA, SAE AIR6127 studies arc and electric discharge up to 1.5 kV, but AEA EPS will be beyond the studied voltage [26]. Nonetheless, the analysis performed in [26] shows that based

This article has been accepted for publication in a future issue of this journal, but has not been fully edited. Content may change prior to final publication. Citation information: DOI 10.1109/TTE.2021.3052106, IEEE Transactions on Transportation Electrification

on Paschen's law [27] for aerospace application, conductors and power electronics in general will required much larger insulation, which is translated in additional unwanted weight and volume.

Although greener solutions imply achieving advantages over traditional aircrafts, because the design constraints mentioned the specific power and power density of the EPS building blocks needs to be increased. The minimum EPS specific power and efficiency values required to outperform conventional gas turbine system has been presented in [28] for a 50% fuel burn reduction on an all turboelectric case. In this work those requirements are going to be set as target points for all the architectures. Therefore, specific power and efficiency requirements for a 20 MW AEA are 7.5 kW/kg and 93%, respectively.

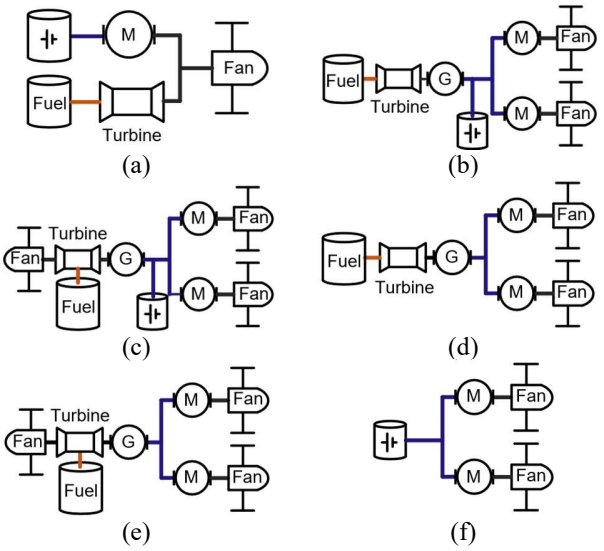

Fig. 3. High level schematics of AEA architectures Power conversion stages are ignored. (a) Parallel hybrid. (b) Series hybrid. (c) Series/Parallel hybrid. (d) All turboelectric. (e) Partial turboelectric. (f) All electric.

Current efforts include increasing the switching frequency, evaluation of new materials, new semiconductor devices and cooling solutions. Integration of power converters within the propulsion motors and generators is becoming attractive to save weight [29]. High power and high voltage under aircraft boundary conditions will require power modules with high switching speed, high voltage ratings and high operation temperature. Wide-bandgap (WBG) technology is a good candidate to expand actual limits of semiconductors power and voltage ratings although drop-in replacement of traditional Si based topologies creates complications.

Current trends in electrical aircrafts discuss the use of superconductive and/or cryogenic cooled approaches to reduce the high losses in MW level architectures and improve power density of the whole EPS [30]–[36]. However, superconducting architectures still present several drawbacks and challenges. For instance, to achieve superconductive materials a cryogenic cooling system is required impacting size, weight, efficiency and specific power [37]–[39]. In addition, due to the novelty there is no clarity when it comes to the operation of such devices at high altitude.

The study carried out in this work will perform a high level study of the different EPS building blocks without delving into the study of the technology. As it has been previously introduced, the criteria to classify the building blocks (i.e., power converters, storage systems, cables, generators and loads) of the EPS are specific power or power density (kW/kg), efficiency and reliability. For instance, Onera, the French Aerospace lab [40], has recently published some results of the DRAGON EU project [41]. Specific power and efficiency of more relevant EPS building block under three evolution levels towards 2035 are presented. Technology assumptions for a significant evolution are sown in Table I. This work will provide an update accounting for recent technological improvements in current technology.

TABLE I
ESTIMATED AEA EPS BUILDING BLOCKS SPECIFICATIONS TOWARDS 2035

Building Block	Specific Power or Specific weight	Efficiency
Generator	19 kW/kg	98.00 %
Motor	25 kW/kg	99.00 %
Inverter	25 kW/kg	99.00 %
Cable	0.5 kg/m	99.60 %
Circuit Protection	100 kW/kg	-

In summary, this work contributes to the analysis and comparison of the most promising propulsion architectures for AEA EPS. Both dc and ac distribution architectures are studied to understand which distribution is best. Dc distribution has been gaining popularity due to the amount of dc loads and weight benefits as demonstrated for shipboard power systems [42]. In the case of ac, the introduction of ac-ac converters reduces the number of conversion steps and benefits in weight and efficiency are expected. However, high altitude effects taking place could potentially eclipse these advantages, and careful evaluation and trade-off as proposed in this work is required.

This paper is structured in the following sections. Section II defines the design requirements and the FoM to be considered for comparison purposes of this analysis. In Section III, the discussion focuses on the FoM calculation methods and the simplifications and assumptions which have been used. Section IV and V evaluate AEA EPS architectures for dc and ac distribution, respectively. Finally, a discussion is performed in the last section stating the conclusions that can be extracted of this work and the required future developments on these topics.

II. DESIGN REQUIREMENTS

The analysis to be carried out in this work will be focused on narrowbody passenger aircraft class architectures taking into account that they are the main contributor of CO2 emissions related to commercial aircraft. The paradigm shift when moving from MEA narrowbody to AEA requires to reconsider voltage and power levels to make this effort fruitful. Based on the current power required the estimated electrical power to properly operate an AEA narrowbody, such as the A320, would be around 20 MW [28]. It is worth noting that distributed propulsion is highly regarded in electrical aircraft to enhance

This article has been accepted for publication in a future issue of this journal, but has not been fully edited. Content may change prior to final publication. Citation information: DOI 10.1109/TTE.2021.3052106, IEEE Transactions on Transportation Electrification

the fuselage aerodynamics [43], [44] However, distributed propulsion negatively impacts power, weight and volumetric requirements for the electric system [45]. The evaluation of this kind of propulsion systems would require the use of Model Based Systems Engineering (MBSE) analysis [46], [47] to correctly identify the benefits in terms of weight at system level. This is out of the scope of this work. Thus, all the analysis is going to focus on the electrical architecture of a twin-propeller A320 based aircraft.

Current trends on high voltage operation of aircraft study voltages above 1 kV, where 3 kV can be considered as a potential new standard if the E-FANX project is assumed as reference [20]. For simplicity in this work, 3 kV is selected as the dc distribution voltage, and ac distribution voltage is established as the equivalent rms line to line 3 kV rectified voltage under SPWM modulation and maximum modulation index, it is $\frac{Vdc}{\sqrt{2}}$.

Aside from the voltage distribution the figures of merit: reliability, specific power, and efficiency need to be carefully studied. Particularly for reliability a certain FIT rate will need to be ensured to comply with the regulation and will be set in the analysis as a mandatory condition (i.e., all EPS proposals must satisfy the reliability requirement). As regards the other FoMs, a correlation exists between them requiring the definition and estimation of all the building blocks within the architecture (e.g., a dc-dc converter can be made extremely power dense, but its efficiency and reliability may suffer in the process.). Details about the three FoMs design requirements are given in the following paragraphs. It should be noted that voltage and current levels will impact the aforementioned FoMs for the building blocks, but for the sake of simplicity the average and a 3 kV dc or ac bus will be considered as a matter of example, even if the actual analysis considers all different voltage and current levels.

TABLE II
DO-254 DESIGN ASSURANCE LEVELS (DALS)

Design Assurance Level (DAL)	**Description**	**Target System Failure Rate**
Level A (Catastrophic)	Failure causes crash, deaths.	$< 10^{-9}$ chance of failure/flight-hr.
Level B (Hazardous)	Failure may cause crash, deaths.	$< 10^{-7}$ chance of failure/flight-hr.
Level C (Major)	Failure may cause stress, injuries.	$< 10^{-5}$ chance of failure/flight-hr.
Level D (Minor)	Failure may cause inconvenience.	No safety metric.
Level E (No effect)	No safety effect on passengers or crew.	No safety metric.

Design Assurance Guidance for Airborne Electronic Hardware (DO-254) is a formal safety standard that provides guidance for design assurance of all inboard electronics of an aircraft. It classifies hardware equipment into five levels of compliance (from A to E) depending on the failure effect in the aircraft operation. They are displayed in Table II.

In the case of the EPS architecture main hardware failure is allocated in the most stringent category, defined as Level A or Catastrophic event. Additionally, special abnormal operation conditions can be set from actual regulation [48]–[50] or pilot guides [51]. Following those indications, in this study the EPS architecture hardware catastrophic effect failure will be defined as all possible events that could reduce EPS power generation under 1/3 of the whole aircraft EPS rated power (i.e., failure occurs if the available power is less than 6.67 MW), being allowed single engine operation. This power is assumed as the minimum power required to continue flying at 200 nmi and to perform an emergency landing.

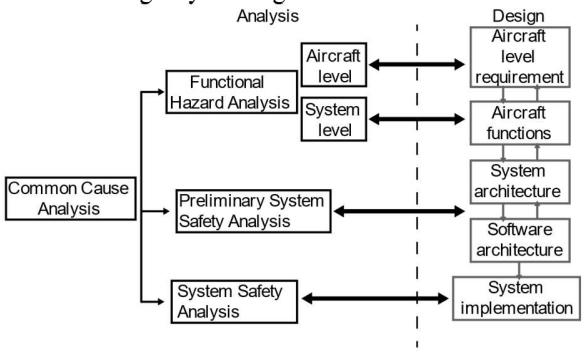

Fig. 4. Representation of the SAEARP4761 security processes.

Aircraft systems reliability is a complex endeavor from the initial design stage until the final certification. For the sake of simplicity, SAE ARP4761 recommended practices guidance has been followed in this work. Fig. 4 shows a block diagram summarizing the process [52]. This work has carried out both Functional Hazard Analysis (FHA) and Preliminary System Safety Analysis (PSSA) of the EPS. In accordance with FHA, DO-254 Level A failure potential causes have been identified. PSSA aim is to identify the needed redundancy to fulfill reliability requirements.

TABLE III
EPS BUILDING BLOCKS SPECIFICATIONS.

Failure rate [FITs]		Specific Power [kW/kg]	Efficiency [%]
Motor	30000	21	96.00
Inverter	1100	37	99.50
Cable*	60	-	-
Generator	30000	21	96.00
Rectifier	1100	49	99.00
Fuel Cell	45000	5	60.00
Battery	4500	700**	60.00
dc-dc	3000	62.5	99.00
CBs	1	31	99.50

(*) Cable specific power and efficiency are calculated based on a conductor model presented later in this paper. (**) Energy density [W.h/kg].

Individual EPS architecture building blocks FoMs have been estimated with a 10-year horizon based on expected technology progression. A summary of these estimations is displayed in Table III. This data is presented as the average of all the results obtained for a range of operation conditions (i.e., range of voltages and currents). The information related with the specific power include packaging and cooling penalization factors. This information serves to enhance the data previously shown in Table I.

This article has been accepted for publication in a future issue of this journal, but has not been fully edited. Content may change prior to final publication. Citation information: DOI 10.1109/TTE.2021.3052106, IEEE Transactions on Transportation Electrification

Table III summarizes the expectations for technologies in the futures years [53]–[55]. In the case of electric machines non-cryogenic solutions such as permanent magnet synchronous machines and high temperature superconducting (HTS) machines were considered. Fuel cell analysis studies proton exchange membrane (PEM), as it is the most mature technology, and also solid state oxide fuel cells as a more disruptive technology. Metal air and lithium air technology are the most promising battery solutions in terms of power density and therefore of interest for their implementation in aircraft applications. Regarding protection devices, solid state protection circuits (SSPCs) are considered a clear candidate to substitute conventional circuit breakers in MW applications [56]. From SoA technology, such as [57], technical specifications could be extrapolated. Power electronics analysis was carried out taking into account three-level inverters/rectifiers and three-level bidirectional boost/buck converters using next generation Silicon Carbide (SIC) for the switches [58].

III. FoM CALCULATIONS

Before starting the description on how each FoM has been estimated the assumptions taken need to be described:

- Reconfiguration is not considered for reliability concern (i.e., elements only have one active stage, for instance, power converters have not a degradation mode which allows them to continue working if they lose a leg).
- Only stand-by redundancy is assumed. Spare unit idle failure rate is considered for the switch and the Fail to Run (FTR) or Fail to Start (FTS).
- Only "Open stage" failure mode is evaluated.
- Propellers, turboshaft or turbofan elements are not included in the analysis. The analysis is focused only on the electrical system.
- In case there are 'n' power sources, it is considered all are designed for giving the minimum required propulsion power in abnormal operation (i.e., 1/3 of the total power).
- Power sources are excluded from EPS architecture efficiency calculation.

FoMs calculation follows the calculation methodology described by Fig. 5 flow chart.

For PSSA analysis, Fault Tree Analysis (FTA) has been used. In [59], a similar validation method based on FTA has been performed for Boeing 747 aircraft subsystems. Additionally, FTA analysis has been based on the weakest-link technique, which consists in identifying the element or subsystem with the highest failure rate (i.e., weakest-link) and then improving its reliability by applying redundancy. An example is illustrated in Fig. 6.

Reliability of elements with spare units can be good approximated by the first 'n' terms of the Poisson expression,

$$R(t)_{system} = \sum_{i=1}^{n} \left(e^{-\lambda * t} \cdot \frac{\lambda * t^{i-1}}{(i-1)!} \right), \qquad (1)$$

being 'n' the total number of elements and 'λ' the failure rate expressed in "failures/hr." and 't' the flight time in seconds [60]. However, it is worth noting that this calculation method ignores the failure of the standby element before running.

A better approach is made by using a "Priority AND gate" that imposes an AND gate condition with specific execution order among its inputs, see Fig. 6.b. Thus, reliability of elements with spare units can be modelled with this gate, where the inputs are the active and the standby units. The spare unit reliability is defined with an OR gate which inputs, in this case, are the following three events: a) Automatic switch fails to switch on demand to start standby component; b) Standby element FTS given successful operation of the automatic switch; c) Standby element fails during running (FTR) after successfully substituting the failed element.

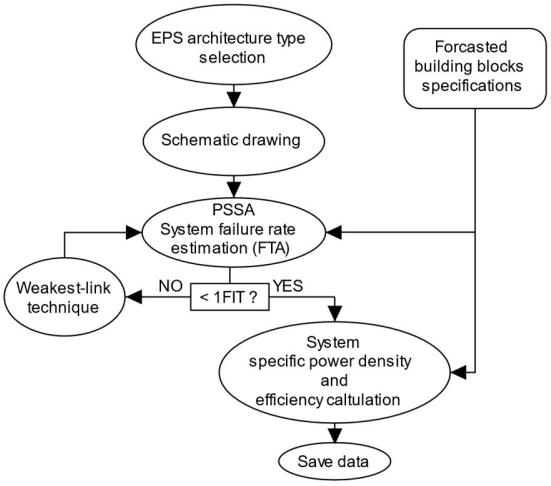

Fig. 5. FoM calculation flow chart.

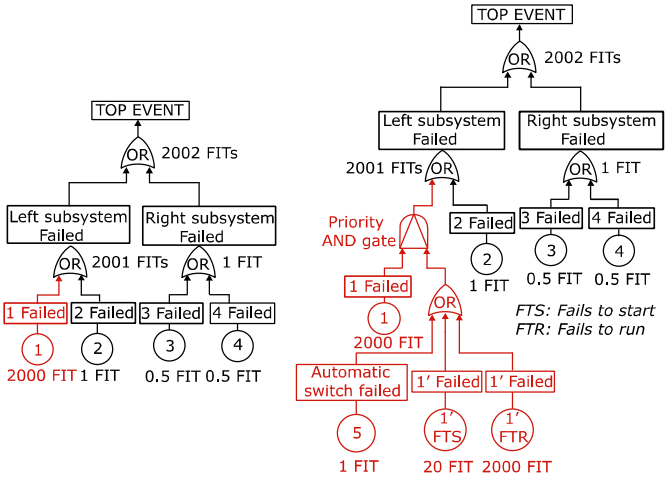

(a) (b)

Fig. 6. Example of application of the weakest-link technique. (a) Fault tree model of a system with one component representing the weakest link (highlighted in red). (b) Fault tree model with a standby component represented by a logical "Priority AND' Gate (highlighted in red).

As shown in Fig 6.b, adding the standby component results in lowering the failure rate of the system (Top event) from 2000 to 2 FITs.

Following the steps defined in Fig. 5, once redundancy

This article has been accepted for publication in a future issue of this journal, but has not been fully edited. Content may change prior to final publication. Citation information: DOI 10.1109/TTE.2021.3052106, IEEE Transactions on Transportation Electrification

requirements are fulfilled at architecture level, specific power density and efficiency are calculated for future comparison. System specific power is given by,

$$\rho_{\text{system}} = \frac{P_{\text{total}}}{W_c + \sum W_x}, \quad (2)$$

where P_{total} is the EPS architecture total power. "W_x" is the weight of each EPS architecture building block except the transmission cable, which is represented by "W_c". "W_x" is computed assuming Table III average power density (ρ_x) times the building block power rate (P_x),

$$W_x = \rho_x P_x. \quad (3)$$

Cable weight comes from the addition of the conductor and the insulation weight,

$$W_c = W_{cond} + W_{insul}. \quad (4)$$

The conductor is sized following the design method presented in [61], where the conductor diameter is computed based on thermal limitations. The resultant conductor mass expression (W_{cond}) can be simplified as

$$W_{cond} = K_{cond} L_{cond}, \quad (5)$$

being "K_{cond}" a constant that depends on the power flowing through the transmission line (P_{cab}), the dc voltage (V_{DC}), the maximum current density (J_{cab}) for a maximum operation temperature, the specific gravity of the conductor material (ρ) and a multiplication factor that is equal to 2 in the case of dc distribution and $\frac{\sqrt{6}}{\cos(\varphi)}$ for ac systems (being $\cos(\varphi)$ the power factor). "L_{cond}" is the cable length.

Insulation weight (W_{insul}) is given by the insulation thickness needed and the length of the cable. As have been aforementioned in the Section I, AEA power ratings, frequency and high altitude conditions make it a unique application when compared to other installations of similar voltage or power levels. In fact, current space high voltage cable technology may not be suitable. For instance, GORE High voltage cables [62] cover up to 36 kV but their design is focused on spaceflight applications and therefore they are mainly designed for vacuum conditions.

For these reasons, the insulation is going to be calculated based on extrapolating aerospace cables specifications, by using the insulation thickness of terrestrial cables as a baseline. From these analyses an empirical relation between the thickness and the voltage level is yielded as,

$$r_{ins\_out} = 0.25 V_{DC} + 1.3. \quad (6)$$

The insulation weight (W_{insul}) is calculated based on the insulation volume and an insulation material density, ρ_{insul}, equal to 1400 kg/m^3

$$w_{insul} = A_{insul} \cdot \rho_{insul}. \quad (7)$$

The global system efficiency is defined as the ratio between the real useful power and the generated power,

$$\eta_{\text{system}} = \frac{P_{useful}}{P_{useful} + Losses}. \quad (8)$$

The generated power is computed as useful power plus system losses, which are defined as (8). Please note that system losses (9) are broken down into cable losses and building block losses, (10) and (11) respectively.

$$\text{Losses}_{\text{system}} = \text{Losses}_c + \sum Losses_x. \quad (9)$$

Transmission line losses (Losses_c) are defined as the total EPS conductor joule losses. Ac and dc cable resistance is obtained from [61] transmission line model.

$$\text{Losses}_c = Losses_{DC} + Losses_{AC} = \sum \left(R_{DC} {I_{DC}}^2\right) + \sum \left(3 R_{1\phi} {I_{1\phi}}^2\right). \quad (10)$$

Building block losses (Losses_x) are calculated with the estimated average efficiency, given by Table III, assuming it remains constant for the whole power range,

$$\text{Losses}_x = (1 - \eta_x) P_x. \quad (11)$$

IV. DC DISTRIBUTION ARCHITECTURE ANALYSIS

In EPS architectures the integration of power electronics with the electric motors and generators is considered as a promising approach to decrease system weight. The ac transmission line length can be reduced, and therefore the cable weight by using dc distribution to the motor end, see Fig. 7 .b.

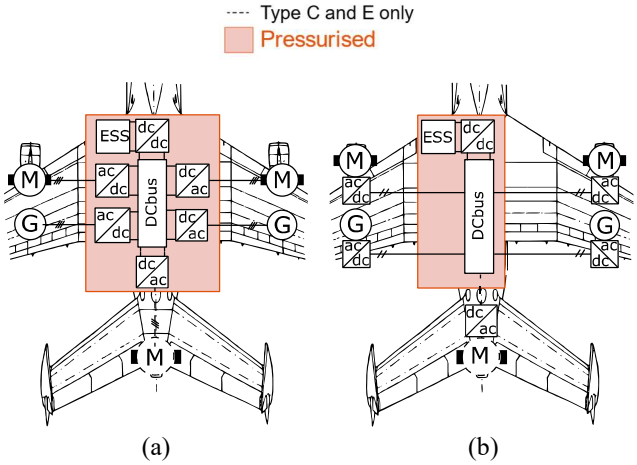

Fig. 7. Potential EPS building blocks location in the aircraft for power electronics. (a) Installed in the pressurized cabin and (b) integrated within the electric machines

From the definition of conductor mass given and explained in Section III, it can be deduced that even assuming unity power factor (i.e., the most beneficial situation for ac cable) ac transmission line mass is approximately 20% higher than a dc transmission line, assuming the same cable material and length. Thus, power electronics integration with the electric machines leads to a trade-off between power electronic design complexity (i.e., safety design) and weight reduction. Power electronics design complexity is dramatically increased because of the tough environmental conditions (i.e., present of loads of noise, un-pressured environment, dirt, etc.)

This article has been accepted for publication in a future issue of this journal, but has not been fully edited. Content may change prior to final publication. Citation information: DOI 10.1109/TTE.2021.3052106, IEEE Transactions on Transportation Electrification

A set of 17 dc EPS architectures has been analyzed based on the future propulsion systems shown in Fig. 3 and the design requirements defined in section II. All of them have been design giving priority to the reliability by ensuring the reliability requirement is fulfil at system level.

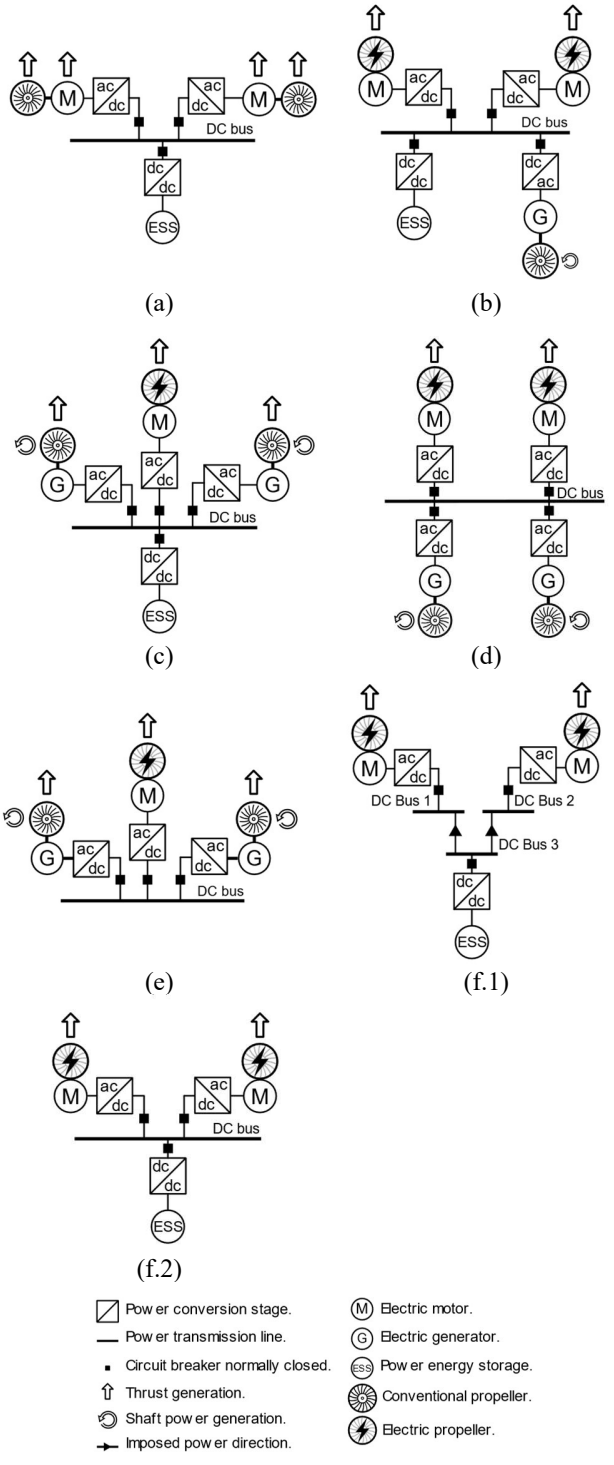

Fig. 8 Diagrams of dc EPS architecture: a) Type A cases, parallel hybrid architecture (A), b) Type B cases, series Hybrid architecture (B), c) Type C cases, series/Parallel hybrid architecture (C), d) Type D cases, all turboelectric (D), e) Type E cases, partial.

Table IV presents a brief description of all dc EPS study cases and Fig. 8 shows simplified diagrams of the EPS architecture types under study. It should be noted that the EPS architecture type is related with the EPS labels presented in Fig. 3. Since A320 aircraft has been taken as a reference, all EPS cases are designed considering a twin propulsion configuration. Electric motors and generators are assumed to be located under the wings (i.e., next to the propellers).

TABLE IV
BRIEF DESCRIPTION OF THE STUDY CASES

Type	ID	Description	Ref.
A	A1	Electric propulsion system is rated at 2/3 of the total power. Fuel cell is used as ESS.	[18], [19]
	A2	Electric propulsion system is rated at 5/6 of the total power. Fuel cell is used as ESS.	
	A3	Electric propulsion system is rated at 2/3 of the total power. Li-Ion battery is used as ESS.	
	A4	Electric propulsion system is rated at 5/6 of the total power. Li-Ion battery is used as ESS.	
B	B1	One turboshaft moves one generator. Two independent fuel cells are used to assist peak power demands.	[20]
	B2	One turboshaft moves one generator. Three independent fuel cells are used to assist peak power demands. Main DC bus is split in two, the fuel cells can supply power to either or both of them but power flow from one to another is forbidden.	
C	C1	STARC-ABL concept plus fuel cell as ESS. 1/3 of the propulsion is provided by tail propeller.	[22]
	C2	STARC-ABL concept plus fuel cell as ESS. 2/3 of the propulsion is provided by the tail electric propeller.	
	C3	STARC-ABL concept plus battery as ESS. 1/3 of the propulsion is provided by the tail electric propeller.	
	C4	STARC-ABL concept plus battery as ESS. 1/3 of the propulsion is provided by the tail electric propeller.	
D	D1	Two turboshafts drive two generators.	[21]
	D2	Two turboshafts, each one drives two independent generators (1/3 and 1/6 rated power).	
E	E1	STARC-ABL concept. 1/3 of the propulsion is provided by the tail electric propeller.	[22]
	E2	STARC-ABL concept. 2/3 of the propulsion is provided by the tail electric propeller.	
F	F1	Three independent fuel cells supply the power. Main DC bus is split in two, the fuel cells can supply power to either or both of them but power flow from one to another is forbidden.	[23], [24]
	F2	Two independent fuel cells supply the power to two electric fans.	
	F3	Three independent fuel cells supply the power to two electric fans.	

This article has been accepted for publication in a future issue of this journal, but has not been fully edited. Content may change prior to final publication. Citation information: DOI 10.1109/TTE.2021.3052106, IEEE Transactions on Transportation Electrification

Circuit breakers have been placed following a fault-isolation strategy similar to those used in ship microgrid [42]. In EPS types C and E, a third motor is located in the aircraft tail following STARC-ABL propulsion system configuration [22]. Fig. 9 provides the dimensions used for cable length estimation.

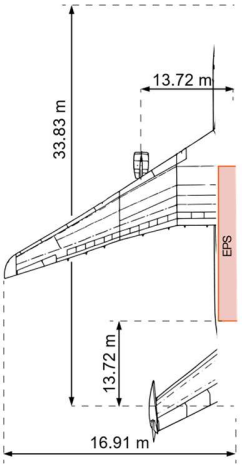

Fig. 9. Main aircraft measurements considered for the study.

Because of the weight reduction, the studied dc EPS architectures are based on Fig. 7.b. For comparing dc EPS architectures, a third index has been added to the three FoMs: fuel dependency. Fuel dependency index has been defined as the percentage of the total power that directly (i.e., conventional propellers) or indirectly (i.e., turboshaft) is produced by fuel burn.

The evaluation of the 17 cases follow the flow chart described in Fig. 5 and FoM equations given in section III. The study has been performed for a generic flight profile for a CS-25 aircraft operating during an hour and a half, considering climb, cruise and descent phase for a full power operation of 20 MW reaching an altitude at cruise of 25000 ft. Efficiency (red), fuel dependency (blue) and specific power (green) results of all the dc EPS cases have been represented in Fig. 10. From left to right it can be seen the data obtained for parallel hybrid, series hybrid, series/parallel hybrid, all turboelectric, partial turboelectric and all electric cases. Table V summarizes the data included in the diagram. Additionally, Table VI presents details about the weight and losses calculations for B1 series hybrid study case as a matter of example. Firstly, Fault Tree Analysis (FTA) reported the need of redundancy in the dc bus. This affects the total weight of the system. The resulted total weight and losses are 6339.33 kg and 1496.73 kW respectively. With equations (2) and (8) specific power and efficiency values displayed in Table V are obtained.

Looking at the specific power FoM (green), hybrid parallel systems A3 and A4 and series/parallel hybrid system C3 and C4 are the heaviest EPS architecture solutions. Those cases have been designed assuming future Li-Air battery technology with an energy power density of 700 W.h/kg and an energy capability to supply 20MW during 1.5 hours. It has been concluded that even with the expected batteries technologies future improvements, hybrid propulsion EPS architecture`s specific power density is significantly penalized.

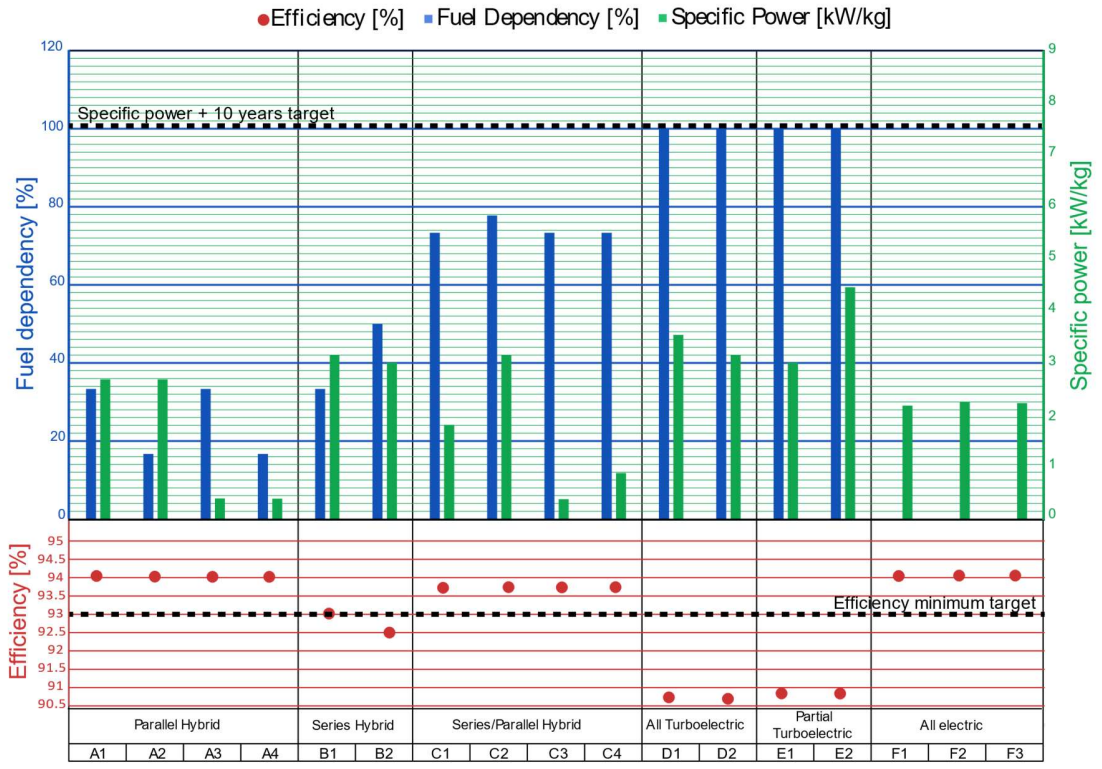

Fig. 10. Specific power density, efficiency and fuel dependency results for all study cases.

This article has been accepted for publication in a future issue of this journal, but has not been fully edited. Content may change prior to final publication. Citation information: DOI 10.1109/TTE.2021.3052106, IEEE Transactions on Transportation Electrification

TABLE V
NUMERICAL RESULTS OF FIG.10. DC EPS ANALYSIS FOM RESULTS.

FoM	Efficiency [%]	Fuel dependency [%]	Specific power [kW/kg]
A1	94,16	33,33	2,71
A2	94,16	16,67	2,71
A3	94,16	33,33	0,43
A4	94,16	16,67	0,43
B1	93,04	33,33	3,15
B2	92,45	50,00	3,02
C1	93,62	73,33	1,79
C2	93,62	77,78	3,14
C3	93,62	73,33	0,40
C4	93,62	73,33	0,78
D1	90,60	100,00	3,46
D2	90,57	100,00	3,16
E1	90,68	100,00	3,05
E2	90,68	100,00	4,41
F1	94,14	0,00	2,56
F2	94,15	0,00	2,30
F3	94,14	0,00	2,29

In terms of efficiency, depicted in red in Fig. 10, the all electric EPS architectures cases with fuel cells exhibit the highest efficiency (i.e. less conversion stages from generation to motors reduce the losses) and a zero-fuel dependency. However, they are the next heavier cases with an average estimated specific power density of 2.3 kW/kg. It is worth noting that the all electric cases present future fuel cell technologies, which include a small battery for stability and fast transient reaction, as ESS and that this value would be lower if only batteries would have been used instead (i.e., lower than 1 kW/kg). Therefore, it can be concluded that even though the ideal solution, in terms of CO_2 emissions, would be full electric propulsion, ESS technologies, even fuel cells, will not be prepared in a short-medium term to make all electric EPS architectures a reality in narrowbody aircrafts. Instead, hybrid systems using fuel cells or turboelectric EPS architectures seems to be more suitable candidates. Partial turbo-electric system (E2) achieves a high specific power density. However, system efficiency drops under 91%. and system is totally dependent of fuel burn. The turboelectric concept is based on the idea of reducing the fuel consumption, by improving the aircraft efficiency, and could be a good solution during the transition from MEA to AEA or other aircrafts types, such as future widebody aircrafts, which perform longer missions.

Based on the analysis, the most promising EPS architectures are those that reach a good trade off among the three FoM. Parallel hybrid and series hybrid EPS architectures, using fuel cell as ESS are the four cases with best performance (i.e., A1, A2, B1 and B2), Fig. 10. They present high efficiency that is in most of the cases above the minimum target of 93% and a reduction of at least a 50% on the use of fuel. Nevertheless, the achievable specific power drops far from the set target of 7.5 kW/kg indicating the necessity of a major technological challenge to happen in the next 10 years. However, in the context of the current work the target is comparing and finding out the most promising EPS architectures that can reduce the CO_2 emissions by increasing the electrification effort on the aircraft, and consequently, lowering fossil fuel dependency. Series and parallel hybrid EPS architecture have a low fuel dependency due to the introduction of batteries and fuel cells. In the case of parallel hybrid, the electric motors powered by the ESS will provide most part of the thrust reducing the size of conventional turbines. In series hybrid, the battery will provide most part of the power so the fuel utilized to power up the generator will be reduced. A lower size turboshaft can be translated into lower fuel dependency of the EPS architecture. Furthermore, those turboshafts can be operated more efficiently in the case of series hybrid. In parallel hybrid systems the turbofans only operate during peaks of power demand (e.g., take off or transitions) [18].

TABLE VI.
B1 SERIES HYBRID CALCULATION DATA EXAMPLE

		Specific power [kW/kg]	Efficiency [%]	Total Power [kW]	Total length [m]	Total weight [kg]	Power Losses [kW]
		Table III		*Table IV*	*Fig.9*	*Eqn. (3)-(5)*	*Eqn. (9)-(11)*
Building Blocks	**Motors**	21	96.00	20000	-	952.38	800
	Inverters	37	99.50	20000	-	540.54	100
	Generator	21	96.00	6667	-	317.46	266.67
	Rectifier	49	99.00	6667	-	136.05	66.67
	Fuel Cell	5	60.00	13333	-	2666.67	*Not considered*
	dc-dc converter	62.5	99.00	13333	-	213.33	133.33
	Circuit breakers	31	99.50	20000	-	1290.32	100
	Dc able	-	-	-	47.16	199.	30
	Ac cable	-	-	-	3	23.48	
Subsystems	**Propulsion**					1492.92	-
	Power source					3333.51	
	Distribution					222.58	
	Protection					1290.32	
	Total					6339.33	1496.73

This article has been accepted for publication in a future issue of this journal, but has not been fully edited. Content may change prior to final publication. Citation information: DOI 10.1109/TTE.2021.3052106, IEEE Transactions on Transportation Electrification

V. AC DISTRIBUTION ARCHITECTURE ANALYSIS.

The second part of the analysis focuses on ac EPS architectures. In this kind of EPS, ac-ac converters become a key piece. The main functions of ac-ac converters are to drive the electric motors and to interconnect two different ac networks. However, ac-ac converters, such as matrix or back to back converters, were not analyzed in the building block study presented in TableTABLE III. Therefore, for ac EPS architectures study, first it has been evaluated the specific power and efficiency requirements of ac-ac converters.

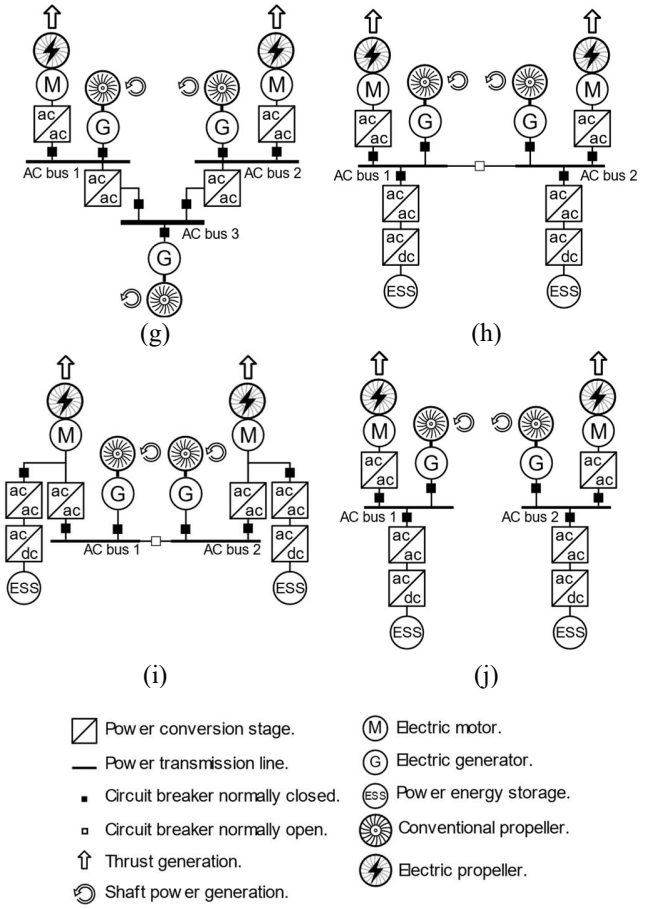

Fig. 11. Diagrams of ac EPS architecture: g) Case G, full turboelectric, baseline case, h) Case H, ESS merged with generators and interconnected buses, i) Case I, direct ESS assistance to motor, ac-dc converter can drive the motor in case of emergency and j) Case J, separated buses with merged ESS.

A simplified scheme of the most relevant ac EPS architectures analyzed can be seen in Fig. 11. Fig. 11.g case is taken as a baseline; it is designed following a full turboelectric propulsion configuration with three generators. The power flow is controlled by ac-ac converters from ac bus 3 to the other two buses avoiding the power flow between buses 1 and 2. From PSSA it has been deduced that three generators increase the reliability of the power source subsystem to the target requirement. For designing Fig. 11.h case, Fig. 11.g has been derived into a series hybrid EPS architecture by replacing the third generator by two ESS units. It is assumed that each ESS is rated to 1/3 of the propulsion power. In normal operation ac buses are working independently but both buses can be connected in case of failure. Fig. 11.i, is similar to Fig. 11.h but ESS is connected to the electric motor terminals with the aim of reducing the ac-ac requirements by decreasing the power managed. Finally, Fig. 11.j explores the influence of buses interconnection elimination considered in Fig. 11.h architecture.

As dc EPS architecture, the same EPS building block average specifications (Table III) have been considered. Equally, the FoMs calculations presented in Section III have been followed. For the ac-ac converter building block specifications a system of equations was solved for each of all the cases imposing the best achievable system requirements (i.e., boundary conditions that provide a valid system solution), it means, the highest possible system efficiency and specific power density, to get ac-ac converter needed requirements. As the most demanding scenario is considered the possibility of having redundancy of any building block is not assumed. Table VII summarizes the results.

TABLE VII
AC EPS AND AC-AC FOM VALUES

Case		G	H	I	J
System	**Failure rate [FITs]**	1	1	1	1
	Specific power [kW/kg]	4.5	2.75	2.7	2.7
	Efficiency [%]	92	93	93	93
ac-ac	**Failure rate [FITs]**	1502	1503	No restricted	1501
	Specific power [kW/kg]	48.47	67.65	43.25	38.23
	Efficiency [%]	99.90	99.61	99.61	99.61

The study concludes that ac-ac converters failure rate should be below 1500 FITs to fulfil DO-254 reliability requirement. It is worth noting that in Fig. 11.c the reliability of the ac-ac is not critical (labeled as no restricted) because the motor can be driven from the ac-dc converter in case of ac-ac failure. In addition, Fig. 11.d reports the most restrictive ac-ac reliability requirement because there is only one possible power flow path from power sources to motor. Additionally, ac-ac converters should achieve a very high efficiency (i.e., higher than 99%) to allow system efficiency to be over the 90%. The double conversion stage needed to integrate ESS in the ac EPS system is the main efficiency penalization. In terms of specific power, the average of all the results, it is 50 kW/kg specific power density, can be set as the target value.

Once the ac-ac converter specifications were estimated a similar analysis to the one performed in the previous section for dc EPS architecture has been carried out. The most promising dc EPS architecture cases have been compared with the ac EPS architecture cases in terms of efficiency, weigh, and fuel dependency. The comparison in weight has been divided in subsystems: propulsions system (i.e., motors and drives), power supply (i.e., generators, ESS and required power conversion stages), distribution network, (i.e., cable and buses) and protections (i.e., breakers). Thus, the building blocks involved into the most significant penalizations in terms of weight for both EPS architecture types can be identified. Particularly, the

This article has been accepted for publication in a future issue of this journal, but has not been fully edited. Content may change prior to final publication. Citation information: DOI 10.1109/TTE.2021.3052106, IEEE Transactions on Transportation Electrification

target value 50 kW/kg ac-ac converter specific power has been used for the comparative study. Fig. 12 presents the three FoMs data, where A1, A2, B1 and B2 are the dc EPS architecture cases and G, H, I and J, the ac EPS architecture cases.

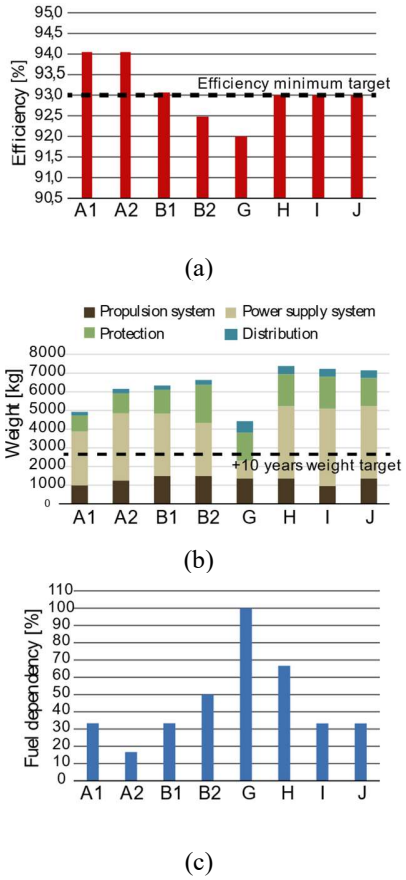

Fig. 12. FoMs comparison between most promising dc cases and ac cases: a) efficiency, b) weight and c) fuel dependency.

Fig. 12.a shows that the dc EPS architecture systems can achieve higher efficiency values than ac EPS architecture systems. In terms of weight, from Fig. 12.b it can be observed that ac distribution weight is higher than dc distribution weight due to cable mass as has been aforementioned. Ac distribution architectures also present heavier power systems (i.e., generators, ESS and needed power converters) when comparing them to dc distribution. One of the biggest drawbacks is the difficulty or the extra power stages required to include ESS making ac distribution not of particular interest for hybrid approaches but particularly interesting for turboelectric architectures. In general, ac EPS systems are heavier than dc EPS systems, the only exception is G because is a turboelectric architecture that does not consider the use of any ESS. In the future for greener aircraft dc distribution systems should prove more useful for either of the distribution cases depicted in Fig. 3 that leverage an ESS.

VI. Conclusions

A comparative analysis on AEA state of art architectures has been presented in this work and has yielded a set of promising EPS architectures that have been compared using three FoMs (i.e., reliability, efficiency and specific power density), and covering both dc and ac distribution systems.

TABLE VIII
ESTIMATION OF BUILDING BLOCK REQUIREMENTS TO FULFIL SYSTEM TARGETS

Case A2	Specific power [kW/kg]		Efficiency [%]	
	Old	*New*	*Old*	*New*
Motor	21	50	96	96
dc-ac	37	60	99.5	99.5
Generator	-	-	96	96
ac-dc	-	-	99	99
Fuel Cell	5	18	100	100
dc-dc	62.5	75	99	99
CBs	31	150	99.5	99.5
System	**2.71**	**7.52**	**94.16**	**94.16**

Case B2	Specific power [kW/kg]		Efficiency [%]	
	Old	*New*	*Old*	*New*
Motor	21	50	96	97
dc-ac	37	55	99.5	99.5
Generator	21	50	96	96
ac-dc	49	55	99	99
Fuel Cell	5	14.5	100	100
dc-dc	62.5	80	99	99
CBs	31	150	99.5	99.5
System	**2.71**	**7.58**	**92.45**	**93.31**

In the case of dc EPS architectures, it has been highlighted the benefits regarding the reduction of cable weight and the ease of implementation for both turboelectric and hybrid propulsion systems. From the analysis, it has been concluded that the parallel hybrid and the series hybrid configurations can be considered promising future aircraft EPS architectures in the medium-term for CO_2 emissions reduction. However, the resultant specific power for those EPS architectures conclude that the 10-year horizon FoM building block estimations do not achieve the fixed target objectives of specific power for narrowbody aircrafts requiring a technological breakthrough in some technologies. Although the main limiting factors is the ESS additional weight, progression of all building blocks technology is needed. Furthermore, circuit breakers lead the system specific power down and are identified as elemental parts in the EPS architecture target achievement. Table VIII displayed an estimation of the building blocks specific power values needed to achieve the system design requirements (i.e., 7.5 kW/kg specific power and 93% efficiency) for the cases A2 and B2.

The conclusion is that a new paradigm of power electronics, insulation conductors and electric machines technologies needs to be explored. Insulation requirements can be highlighted as critical with power density requirements. Nowadays, the effort of many AEA designers is focused on the pursuit of insulation technologies that address high voltage phenomena without penalizing size or weight. It can be done by adapting terrestrial insulation materials or with alternative solutions such as, micro-multilayer insulation technology [63].

The challenge for electric machines design is to achieve high specific power solutions with high efficiency considering current technologies seem to have reach the physical limit. The study presented in [64] analyses electric machines design for

AEA application. The impact of several design parameters on the power density and the efficiency is explored for non-superconducting and superconducting machines. This study demonstrated that superconductivity materials allow to go beyond non-superconducting achievable specific power ratings but at the same time it introduces extra complexity to the design.

Thermal management becomes an important concern for achieving the power density requirements needed in new aircraft propulsion concepts. In conventional aircrafts the heat power produced by the propulsion system is evacuated through the turbine. But, in AEA EPS a thermal management system has to be incorporated to deal with heat power produced by the power train and mainly by power converters. Some authors propose cryogenic cooling and thermal management system integration [65] or the integration of power converters within the propulsion motors to use the bypass flow in the duct to cool the power modules [66].

Conclusions regarding power converter topologies requires a through study and it is considered to be out of the scope of this paper. However, it is worth mentioning that modular or multilevel topologies reduce the power semiconductor requirements and bring AEA EPS power converters requirements closer to state of the art technology. In addition, research on widebandgap devices is critical to improve efficiency and power density.

Technology development will reduce the fuel dependency for these hybrid architectures achieving higher specific power densities and eventually transitioning into a full green electrical system. The significant weight addition of battery ESS as a main source, such as Li-Air (i.e., expected battery technology used in 2030) demotivates their application in the future narrowbody AEA unless a breakthrough technology is discovered to improve their energy density for the power levels discussed in this work. Lighter aircrafts pertaining to EASA CS 23 classification may still benefit from battery use on the lower power end [67]. For instance, over the last years several projects around light aircrafts that propose all electric EPS architectures have been presented [23], [24]. As regards ac EPS architectures, it has been assumed that ac-ac converters must achieve a high-performance (i.e., very high reliability, over 99% efficiency and high specific power density). These requirements stress the design of this component making it extremely difficult to achieve the requirements and thus falling short in comparison to simple dc EPS architectures.

Note that the conclusions expounded above are based on an analysis focused on narrowbody aircrafts. Although, similar analysis could be applied to other types of aircrafts the conclusions expounded may differ due to the characteristics of flight profiles, altitude, distances, or flight time. Several projects around widebody aircrafts can be found, which focus on turboelectric propulsion architectures, such as N3-X prototype [68]. In that case, the fuselage aerodynamic performances become more important, benefiting from distributed propulsion architectures. This EPS architecture presented in [68] combined with innovative superconducting electrical systems can supposed around a 70% of fuel burn reduction.

The benefits of using dc architecture for either hybrid or fuel electric have been concluded in this work. Nonetheless, in terms of the required building blocks there are several technological gaps such as: understanding of high altitude and high voltage operation, achieving fast and power dense dc breakers, or increasing the overall efficiency of the system. Currently efforts in superconductive systems, special insulation materials and hydrogen fuel cells will be key for the future of greener and electrical aircrafts.

REFERENCES

[1]"IATA Forecast Predicts 8.2 billion Air Travelers in 2037." https://www.iata.org/en/pressroom/pr/2018-10-24-02/ (accessed Sep. 04, 2020).
[2]B. Graver, "CO2 emissions from commercial aviation, 2018," p. 13, 2018.
[3]C. Neta, "Pentagon Fuel Use, Climate Change and the Cost of War Final."
[4]Europäische Kommission and Europäische Kommission, Eds., *Flightpath 2050: Europe's vision for aviation; maintaining global leadership and serving society's needs; report of the High-Level Group on Aviation Research*. Luxembourg: Publ. Off. of the Europe. Union, 2011.
[5]"Welcome to the Clean Sky | Clean Sky." https://www.cleansky.eu/ (accessed Sep. 04, 2020).
[6]CS3PG, "Clean_Aviation_SRIA_R1." http://clean-aviation.eu/files/Clean_Aviation_SRIA_R1_for_public__consultation.pdf (accessed Sep. 09, 2020).
[7]I. Moir, "More-electric aircraft-system considerations," in *IEE Colloquium on Electrical Machines and Systems for the More Electric Aircraft (Ref. No. 1999/180)*, Nov. 1999, p. 10/1-10/9, doi: 10.1049/ic:19990839.
[8]J. Chen, C. Wang, and J. Chen, "Investigation on the Selection of Electric Power System Architecture for Future More Electric Aircraft," *IEEE Transactions on Transportation Electrification*, vol. 4, no. 2, pp. 563–576, Jun. 2018, doi: 10.1109/TTE.2018.2792332.
[9]Robert Thomson, "Aircraft Electrical Propulsion – The Next Chapter of Aviation?" *Think:act*.
[10] CleanSky2, "Hydrogen Powered Aviation report." https://www.fch.europa.eu/sites/default/files/FCH%20Docs/20200507_Hydrogen%20Powered%20Aviation%20report_FINAL%20web%20%28ID%206706035%29.pdf (accessed Sep. 04, 2020).
[11] "IATA Sustainable Aviation Fuel Roadmap 1st," Accessed: Sep. 04, 2020. [Online]. Available: https://www.iata.org/contentassets/d13875e9ed784f75bac90f000760e998/safr-1-2015.pdf.
[12] C. Amy and A. Kunycky, "Hydrogen as a Renewable Energy Carrier for Commercial Aircraft," p. 42.
[13] T. Sibilli, C. Senne, H. Jouan, A. T. Isikveren, and S. Ayat, "Synergistic hybrid-electric liquid natural gas drone: S.H.I.E.L.D," *Aircraft Engineering and Aerospace Technology*, vol. 92, no. 5, pp. 757–768, Jan. 2020, doi: 10.1108/AEAT-10-2019-0211.
[14] H. Schefer, L. Fauth, T. H. Kopp, R. Mallwitz, J. Friebe, and M. Kurrat, "Discussion on Electric Power Supply Systems for All Electric Aircraft," *IEEE Access*, vol. 8, pp. 84188–84216, 2020, doi: 10.1109/ACCESS.2020.2991804.
[15] E. National Academies of Sciences and Medicine, *Commercial Aircraft Propulsion and Energy Systems Research: Reducing Global Carbon Emissions*. Washington, DC: The National Academies Press, 2016.
[16] C. L. Bowman, T. V. Marien, and J. L. Felder, "Turbo- and Hybrid-Electrified Aircraft Propulsion for Commercial Transport," Jul. 2018, doi: 10.2514/6.2018-4984.
[17] S. Adibhatla, S. Garg, S. Griffith, K. Karnofski, N. Payne, and B. Wood, "Propulsion Control Technology Development Roadmaps to Address NASA Aeronautics Research Mission Goals for Thrusts 3a and 4," doi: 10.2514/6.2018-4732.
[18] C. E. Lents, L. W. Hardin, J. Rheaume, and L. Kohlman, "Parallel Hybrid Gas-Electric Geared Turbofan Engine Conceptual Design and Benefits Analysis," in *52nd AIAA/SAE/ASEE Joint Propulsion Conference*, 0 vols., American Institute of Aeronautics and Astronautics, 2016.
[19] K. R. Antcliff and F. M. Capristan, "Conceptual Design of the Parallel Electric-Gas Architecture with Synergistic Utilization Scheme (PEGASUS) Concept," doi: 10.2514/6.2017-4001.
[20] L. Juvé, J. Fosse, E. Joubert, and N. Fouquet, "Airbus Group Electrical Aircraft Program, The E-Fan Project," doi: 10.2514/6.2016-4613.
[21] J. Felder, G. Brown, H. DaeKim, and J. Chu, "Turboelectric Distributed Propulsion in a Hybrid Wing Body Aircraft," *undefined*, 2011. /paper/Turboelectric-Distributed-Propulsion-in-a-Hybrid-Felder-Brown/4eb1e7fcf5470bfd625c2d0904b21099ff0bb70a (accessed Sep. 04, 2020).

[22] J. Welstead and J. L. Felder, "Conceptual Design of a Single-Aisle Turboelectric Commercial Transport with Fuselage Boundary Layer Ingestion," Jan. 2016, doi: 10.2514/6.2016-1027.
[23] "Eviation | Eviation Alice." https://www.eviation.co/ (accessed Sep. 04, 2020).
[24] "magniX," *magniX*. https://www.magnix.aero/ (accessed Sep. 04, 2020).
[25] J. Domone, "The challenges and benefits of the electrification of aircraft." https://www.atkinsglobal.com/~/media/Files/A/Atkins-Corporate/Electrification%20White%20Paper%20-%20digital.pdf (accessed Nov. 26, 2020).
[26] "AIR6127: Managing Higher Voltages in Aerospace Electrical Systems - SAE International." https://www.sae.org/standards/content/air6127/ (accessed Sep. 04, 2020).
[27] G. Galli *et al.*, "Paschen's Law in Extreme Pressure and Temperature Conditions," *IEEE Transactions on Plasma Science*, vol. 47, no. 3, pp. 1641–1647, Mar. 2019, doi: 10.1109/TPS.2019.2896352.
[28] P. Kshirsagar, S. Dwari, J. M. Rheaume, R. Taylor, C. E. Lents, and P. Walsh, "Anatomy of a 20 MW Electrified Aircraft: Metrics and Technology Drivers," in *AIAA Propulsion and Energy 2020 Forum*, 0 vols., American Institute of Aeronautics and Astronautics, 2020.
[29] R. Abebe *et al.*, "Integrated motor drives: state of the art and future trends," *IET Electric Power Applications*, vol. 10, no. 8, pp. 757–771, 2016, doi: 10.1049/iet-epa.2015.0506.
[30] O. Fl and T. J. Haugan, "Air Force Research Laboratory," p. 67, Jan. 2013, [Online]. Available: http://publish.illinois.edu/grainger-ceme/files/2015/04/Electric-Aircraft-cleared-AFRL-2013.pdf.
[31] R. Sugouchi *et al.*, "Conceptual Design and Electromagnetic Analysis of 2 MW Fully Superconducting Synchronous Motors with Superconducting Magnetic Shields for Turbo-Electric Propulsion System," *IEEE Transactions on Applied Superconductivity*, vol. 30, no. 4, pp. 1–5, Jun. 2020, doi: 10.1109/TASC.2020.2974705.
[32] S. Zanegin, N. Ivanov, D. Shishov, I. Shishov, K. Kovalev, and V. Zubko, "Manufacturing and Testing of AC HTS-2 Coil for Small Electrical Motor," *Journal of Superconductivity and Novel Magnetism*, vol. 33, no. 2, 2020, doi: 10.1007/s10948-019-05226-1.
[33] F. Weng, M. Zhang, T. Lan, Y. Wang, and W. Yuan, "Fully superconducting machine for electric aircraft propulsion: study of AC loss for HTS stator," *Supercond. Sci. Technol.*, vol. 33, no. 10, p. 104002, Oct. 2020, doi: 10.1088/1361-6668/ab9687.
[34] M. D. Sumption, "AC Loss of Superconducting Materials- refined loss estimates for very high density motors and generators for hybrid-electric aircraft: MgB2 wires, Coated conductor tapes and wires," in *AIAA Propulsion and Energy 2019 Forum*, 0 vols., American Institute of Aeronautics and Astronautics, 2019.
[35] M. Komiya *et al.*, "Design Study of 10 MW REBCO Fully Superconducting Synchronous Generator for Electric Aircraft," *IEEE Transactions on Applied Superconductivity*, vol. 29, no. 5, pp. 1–6, Aug. 2019, doi: 10.1109/TASC.2019.2906655.
[36] "RRI HTS Wire Critical Current Database." http://htsdb.wimbush.eu/ (accessed Nov. 26, 2020).
[37] P. Song, T.-M. Qu, L.-F. Lai, M.-S. Wu, X.-Y. Yu, and Z. Han, "Thermal analysis for the HTS stator consisting of HTS armature windings and an iron core for a 2.5 kW HTS generator," *Supercond. Sci. Technol.*, vol. 29, no. 5, p. 054007, May 2016, doi: 10.1088/0953-2048/29/5/054007.
[38] J. Palmer and E. Shehab, "Modelling of cryogenic cooling system design concepts for superconducting aircraft propulsion," *IET Electrical Systems in Transportation*, vol. 6, no. 3, pp. 170–178, 2016, doi: 10.1049/iet-est.2015.0020.
[39] A. Perez, "Rotor Cooling Concept for the ASuMED Superconductive Motor," *Materials Science and Engineering*, p. 6, 2018.
[40] Onera, "Research paths for a viable air transport system in 2050." Accessed: Nov. 26, 2020. [Online]. Available: https://www.onera.fr/sites/default/files/recherche/ats_2050-phase1_en.pdf.
[41] P. Schmollgruber *et al.*, "Multidisciplinary Design and performance of the ONERA Hybrid Electric Distributed Propulsion concept (DRAGON)," in *AIAA Scitech 2020 Forum*, American Institute of Aeronautics and Astronautics.
[42] Z. Jin, G. Sulligoi, R. Cuzner, L. Meng, J. C. Vasquez, and J. M. Guerrero, "Next-Generation Shipboard DC Power System: Introduction Smart Grid and dc Microgrid Technologies into Maritime Electrical Netowrks," *IEEE Electrification Magazine*, vol. 4, no. 2, pp. 45–57, Jun. 2016, doi: 10.1109/MELE.2016.2544203.
[43] J. Müller *et al.*, "Design Considerations for the Electrical Power Supply of Future Civil Aircraft with Active High-Lift Systems," 2018, doi: 10.3390/EN11010179.
[44] H. D. Kim, A. T. Perry, and P. J. Ansell, "A Review of Distributed Electric Propulsion Concepts for Air Vehicle Technology," in *2018 AIAA/IEEE Electric Aircraft Technologies Symposium*, 0 vols., American Institute of Aeronautics and Astronautics, 2018.
[45] J. Kim, K. Kwon, S. Roy, E. Garcia, and D. N. Mavris, "Megawatt-class Turboelectric Distributed Propulsion, Power, and Thermal Systems for Aircraft," in *2018 AIAA Aerospace Sciences Meeting*, 0 vols., American Institute of Aeronautics and Astronautics, 2018.
[46] I. Lind and H. Andersson, "Model Based Systems Engineering for Aircraft Systems – How does Modelica Based Tools Fit?" Jun. 2011, pp. 856–864, doi: 10.3384/ecp11063856.
[47] A. K. Jeyaraj, "A Model-Based Systems Engineering Approach for Efficient System Architecture Representation in Conceptual Design: A Case Study for Flight Control Systems," masters, Concordia University, 2019.
[48] *Part I - International Commercial Air Transport - Aeroplanes, 8th ed.*, vol. Annex 6.
[49] "14 CFR Part 121 - OPERATING REQUIREMENTS: DOMESTIC, FLAG, AND SUPPLEMENTAL OPERATIONS," *LII / Legal Information Institute*. https://www.law.cornell.edu/cfr/text/14/part-121 (accessed Sep. 04, 2020).
[50] J. Aalders *et al.*, "14 CFR § 25.121 - Climb: One-engine-inoperative." Accessed: Sep. 04, 2020. [Online]. Available: https://www.law.cornell.edu/cfr/text/14/25.121.
[51] U.S. Department of Transportation, *Airplane Flying Handbook. Chapter 12.* .
[52] "ARP4761: Guidelines and Methods for Conducting the Safety Assessment Process on Civil Airborne Systems and Equipment - SAE International." https://www.sae.org/standards/content/arp4761/ (accessed Sep. 04, 2020).
[53] M. J. Armstrong *et al.*, "Architecture, Voltage, and Components for a Turboelectric Distributed Propulsion Electric Grid," *Final Report*, p. 270, 2015.
[54] K. Haran, "Electric/Hybrid-Electric Drives for Aircraft Propulsion," p. 23.
[55] H. Gui *et al.*, "Review of Power Electronics Components at Cryogenic Temperatures," *IEEE Transactions on Power Electronics*, vol. 35, no. 5, pp. 5144–5156, May 2020, doi: 10.1109/TPEL.2019.2944781.
[56] C. Peng, X. Song, A. Q. Huang, and I. Husain, "A Medium-Voltage Hybrid DC Circuit Breaker—Part II: Ultrafast Mechanical Switch," *IEEE Journal of Emerging and Selected Topics in Power Electronics*, vol. 5, no. 1, pp. 289–296, Mar. 2017, doi: 10.1109/JESTPE.2016.2609391.
[57] "Crouzet. Advanced electrical protections. Electromechanics, Mechatronics, Electronics," p. 23.
[58] J. Wyss and J. Biela, "Optimal Design of Bidirectional PFC Rectifiers and Inverters Considering 2L and 3L Topologies with Si, SiC, and GaN Switches," *IEEJ Journal IA*, vol. 8, no. 6, pp. 975–983, Nov. 2019, doi: 10.1541/ieejjia.8.975.
[59] *The 747 Primary Flight Control Systems Reliability and Maintenance Study*. 1979.
[60] D. J. Smith, *Reliability, Maintainability and Risk: Practical Methods for Engineers*. Elsevier, 2013.
[61] S. H. Teichel *et al.*, "Design considerations for the components of electrically powered active high-lift systems in civil aircraft," *CEAS Aeronaut J*, vol. 6, no. 1, pp. 49–67, Mar. 2015, doi: 10.1007/s13272-014-0124-1.
[62] "GORE Space Cables - Catalog (Traditional Space)." Accessed: Sep. 04, 2020. [Online]. Available: https://www.gore.com/system/files/2019-10/GORE%20Space%20Cables%20-%20Catalog%20%28Traditional%20Space%29_10-28-2019%20%28A4%20Electronic%29_0.pdf.
[63] E. E. Shin, D. A. Scheiman, and M. Lizcano, "Lightweight, Durable, and Multifunctional Electrical Insulation Material Systems for High Voltage Applications," in *2018 AIAA/IEEE Electric Aircraft Technologies Symposium (EATS)*, Jul. 2018, pp. 1–21.
[64] S. Du, J. Tangudu, and P. Kshirsagar, "Analytical Model and Design Space Studies for a non-Superconducting and Superconducting Electric Machine for an Aircraft Application," in *2020 AIAA/IEEE Electric Aircraft Technologies Symposium (EATS)*, Aug. 2020, pp. 1–10.
[65] P. Cheetham, B. Darbha, S. Telikapalli, C. H. Kim, M. Coleman, and S. Pamidi, "Superconducting DC power distribution networks for electric aircraft," in *2020 AIAA/IEEE Electric Aircraft Technologies Symposium (EATS)*, Aug. 2020, pp. 1–7.
[66] G. Wortmann, A. Seitz, and S. Rau, "D4.04 Electric Machinery. Preliminary Design report. Centreline." https://www.centreline.eu/wp-content/uploads/CENTRELINE_SIEMENS_D4.04_R1.0.pdf (accessed Nov. 26, 2020).

[67] "CS-23 Normal, Utility, Aerobatic and Commuter Aeroplanes." Accessed: Oct. 01, 2020. [Online]. Available: https://www.easa.europa.eu/certification-specifications/cs-23-normal-utility-aerobatic-and-commuter-aeroplanes.
[68] G. Brown, "Weights and Efficiencies of Electric Components of a Turboelectric Aircraft Propulsion System," 2011, doi: 10.2514/6.2011-225.